Grid Impedance Shaping for Grid-Forming Inverters: A Soft Actor-Critic Deep Reinforcement Learning Algorithm

Oshnoei, Arman; Sorouri, Hoda; Oshnoei, Soroush; Teodorescu, Remus; Blaabjerg, Frede

Published in:
IPEMC 2024-ECCE Asia - 10th International Power Electronics and Motion Control Conference - ECCE Asia

Publication date:
2024

Grid Impedance Shaping for Grid-Forming Inverters: A Soft Actor-Critic Deep Reinforcement Learning Algorithm

Arman Oshnoei*, Hoda Sorouri*, Soroush Oshnoei†, Remus Teodorescu*, Frede Blaabjerg*
*Department of Energy, Aalborg University, Aalborg, Denmark
Email: aros@energy.aau.dk, hoso@energy.aau.dk, ret@energy.aau.dk, fbl@energy.aau.dk
†Department of Electrical and Computer Engineering, Aarhus University, Aarhus, Denmark
Email: soroush_oshnoei@yahoo.com

***Abstract*—This paper proposed an advanced method for adjusting grid impedance in grid-forming inverters, utilizing the Soft Actor-Critic Deep Reinforcement Learning (SAC-DRL) algorithm. The approach contains a flexible strategy for controlling virtual impedance, supported by an equivalent grid impedance estimator. This facilitates accurate modifications of virtual impedance based on the grid's X/R ratio and the converter's power capacity, aiming to optimize power flow and maintain grid stability. A unique feature of this methodology is the division of virtual reactance into two segments: one adhering to standard control protocols and the other designated for precision enhancement via the SAC-DRL method. This strategy introduces a layer of intelligence to the system, strengthening its resilience against fluctuations in grid impedance. Experimental validations, executed on a laboratory setup, verify the robustness of this approach, highlighting its potential to significantly improve intelligent power grid management practices.**

***Index Terms*—Virtual impedance, power decoupling, grid-forming inverter, soft actor-critic deep reinforcement learning, grid impedance estimation.**

I. Introduction

Integrating distributed generators (DGs) into microgrids marks a paradigm shift in energy systems, emphasizing decentralized control and enhanced resilience. Grid-forming (GFM) inverters play a pivotal role in this integration, ensuring stability and reliable power-sharing, especially in islanded operational modes [1]. These inverters are crucial in transforming the operational dynamics of microgrids, enabling them to operate independently from the central grid and thus providing a more flexible and resilient power supply [2].

The conventional approach to managing this integration employs droop control strategies that emulate the behavior of synchronous generators. This method is essential for controlling microgrids, offering a simple and effective way to maintain system stability and distribute power evenly among various distributed energy resources. By mimicking the characteristics of traditional power systems, droop control provides a familiar framework for grid management [3], [4].

However, these strategies encounter limitations, especially in low-voltage microgrids with small X/R ratios, where an undesirable coupling between active and reactive powers emerges, compromising system stability [5]. This coupling effect can lead to voltage fluctuations and power quality issues, posing challenges to the stable operation of microgrids. These challenges are exacerbated in systems with a high penetration of renewable energy sources, such as solar PV and wind turbines, where the variability in power output can further destabilize the grid.

To overcome these challenges, various control and power decoupling strategies have been proposed. Virtual Impedance Decoupling Strategies (VI-DS) are designed to modify the output impedance of DGs, enabling the independent control of active and reactive powers [6]. By integrating a feed-forward control scheme, VI-DS effectively introduces a virtual impedance, creating either inductive or resistive characteristics in the DG output. This adjustment is achieved through the strategic implementation of a virtual impedance, which involves a series connection of negative resistance and inductance. Such a configuration alters the equivalent impedance between a virtual power source and the point of common coupling (PCC), rendering it inductive [7]. However, its performance is contingent on precise knowledge of the microgrid's structure, making it vulnerable to uncertainties and variations in grid impedance. The Q-V modified droop control method [8] offers an alternative, illustrating effectiveness in inductive conditions but struggling under complex feeder equivalent impedance. Also, closed-loop power decoupling strategies incorporate techniques like impedance droop estimation, small-signal injection, and virtual power source control [9]-[11]. The majority of grid-shaping techniques discussed in the literature rely on accurate knowledge of grid impedance parameters, rendering them less effective in situations where uncertainties arise from variations in grid impedance.

Recognizing these challenges, this paper introduces an innovative control strategy using the Soft Actor-Critic Deep Reinforcement Learning (SAC-DRL) algorithm to tune grid impedance in GFM inverters properly. This method integrates a dynamic virtual impedance control mechanism with an equivalent grid impedance estimator, facilitating precise, adaptive adjustments based on the grid's X/R ratio and the converter's power capacity. This ensures optimal power flow and grid stability, even in the face of impedance fluctuations. A

remarkable aspect of the proposed approach is the division of virtual reactance into two segments, providing standard control protocols with accuracy enhancement via SAC-DRLA, thus adding an additional layer of intelligence and resilience to the system.

II. Configuration of Proposed GFM Inverter setup

In Fig. 1, the configuration of the test system is shown, showcasing a GFM inverter integrated into the grid at the PCC via a three-phase LC filter. The LC filter consists of capacitance C_f and inductance L_f. A three-phase RL branch ($Z_g = r_g + j\omega l_g$) emulates the grid's impedance. The architecture of the GFM inverter includes a voltage source inverter equipped with PI controllers for inner current and voltage regulation in the *dq* reference frame. The active power control loop utilizes the synchronous power controller approach, simulating virtual inertia and providing damping to the system [12], [13]. The voltage of the GFM inverter is regulated through the inclusion of a PI controller within the reactive power control loop. The suggested impedance shaping method incorporates a block for estimating equivalent grid impedance, a block for defining the Virtual Impedance (VI) profile, and a block for the VI system based on SAC-DRL method.

A. Equivalent Grid Impedance Estimation

Traditional power flow models can predict the equivalent impedance of a feeder when the voltage and power metrics at the PCC are available. However, DG control mechanisms rely solely on information about output voltage and power for managing power flows, which restricts the ability to accurately determine the equivalent impedance at the PCC. Adding current sensors at the PCC can provide the necessary data for power analysis, thus facilitating the estimation of the PCC's equivalent impedance [1], [14]. This method, though, does not account for the effects of virtual impedance. Therefore, in this study, the reference voltages from the DG control system ($v^*_{o\alpha\beta}$) are included to accurately estimate the equivalent impedance that consists of the impact of virtual impedance. Active and reactive power values corresponding to the equivalent impedance can be determined through the following calculations:

$$\begin{cases} P_c = \delta v_{b\alpha} i_{o\alpha} + \delta v_{b\beta} i_o \beta \\ Q_c = \delta v_{b\alpha} i_{o\beta} - \delta v_{b\beta} i_o \alpha \end{cases} \tag{1}$$

In this context, P_c and Q_c represent the total power output of the DG system, while $\delta v_{b\alpha\beta} = v^*_{o\alpha\beta} - v_{o\alpha\beta}$ denotes the discrepancy in voltage between the designated reference and the actual output from the DG. $i_{o\alpha\beta}$ refers to the current observed at the PCC. To minimize the impact of the switching frequency on the calculations of P_c and Q_c, low-pass filters are utilized.

Given the system's symmetry and balance, the magnitude of its equivalent impedance can be determined through the following estimation:

$$Z_e = \frac{V^*_{o\alpha}}{I_{o\alpha}} = \frac{V^*_{o\beta}}{I_{o\beta}} \tag{2}$$

The components of resistance and reactance in Z_e, representing its real and imaginary parts, are calculated as follows:

$$R_e = \frac{Z_e P_c}{S_c} \tag{3}$$

$$X_e = \frac{Z_e Q_c}{S_c} \tag{4}$$

where $S_c = \sqrt{P_c^2 + Q_c^2}$ represents the apparent power associated with the system's equivalent impedance.

This proposed method calculates the system's equivalent impedance, Z_e, breaking it down into its resistive (R_e) and inductive (X_e) components. This breakdown facilitates the assessment of the feeder's X/R ratio.

B. Definition of VI profile

The VI profile block specifies the VI profile and the values of its components to achieve the targeted X/R ratio. This is done by considering the estimated grid impedance ($Z_e = R_e + jX_e$) and the power availability from the converter.

The calculation of virtual resistance and reactance (r_{vi} and x_{vi}) is determined as follows:

$$r_{vi} = \gamma R_e \tag{5}$$

$$x_{vi} = \lambda X_e \tag{6}$$

where γ and λ represent the reduction factors, which are established based on the desired X/R ratio and power availability of GFM inverter.

C. SAC-DRL based VI control

The calculation of x_{vi} splits it into two components using a distribution factor μ, leading to $x_{vi2} = \mu x_{vi}$ and $x_{vi1} = (1-\mu)x_{vi}$. The approach for virtual reactance x_{vi} adopts a variable structure strategy, where x_{vi1} adheres to the conventional method, and x_{vi2} employs a SAC-DRL-based method to compensate for unmodeled disturbances and accommodate potential variations in grid impedance. In Fig. 1, $Z_e = R_e + jX_e$ represents the estimated equivalent impedance, while r_{vi} and x_{vi} stand for the components of the VI. The term x_{vi2}, derived via the SAC-DRL algorithm, is combined with x_{vi1} to fulfill the X/R control objectives.

The SAC method is a sophisticated reinforcement learning strategy employing deep neural networks to overcome the constraints of limited dimensionality in states and actions. Compared to the deep deterministic policy gradient technique, capable of managing continuous state-action spaces, SAC achieves faster convergence [15]. Distinct from traditional RL algorithms, where the action-value function focuses on maximizing cumulative reinforcement signals, the SAC method optimizes the entropy of data concerning the state independently. To do this, a soft Bellman function is adopted for the

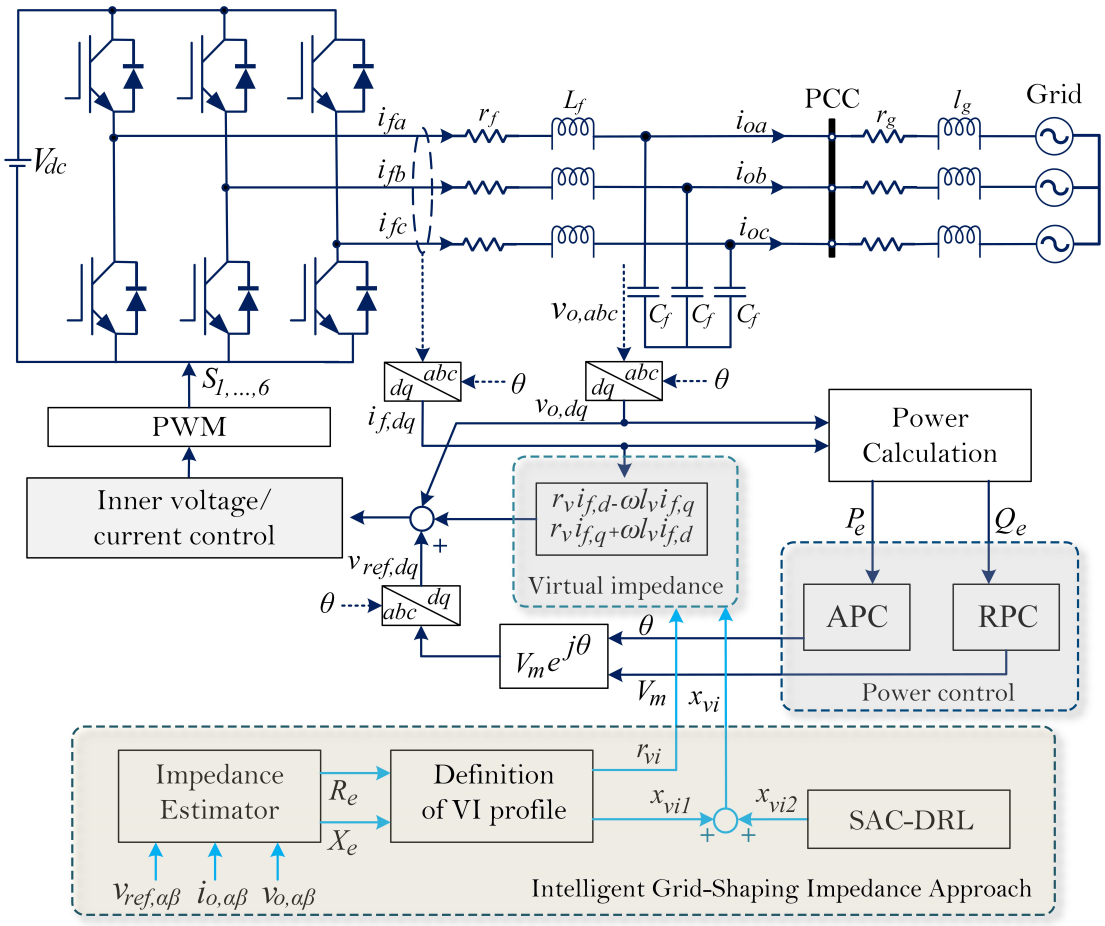

Fig. 1. Block diagram of the proposed GFM inverter setup.

action-value function [16]. The actor-network is designed to generate the best possible actions given the current state of the system. More information on this method is available in [15].

x_{vi2} is the control design parameter adjustable through the SAC-DRL method. Consequently, the action within SAC-DRL is characterized as $a_c = x_{vi2}$. To assess the performance of the SAC's agent, the reward signal is established to reduce the deviation between the reactive power, Q_e, and its set-point value, Q_r. Fig. 2 shows the proposed SAC-DRL-based grid impedance shape implementation.

$$r = \frac{1}{|Q_r - Q_e|} \tag{7}$$

The system state, S_c, receives Q_e as the input for the deep neural networks.

III. Experimental Results

The proposed control strategy was validated using a GFM inverter laboratory setup shown in Fig. 2, configured as per the block diagram shown in Fig. 1. A Cinergia Grid Simulator is used to mimic the power grid. The main parameters of the system are detailed in Table 1. The control system execution and implementation of the SAC-DRLA-based grid impedance shaping algorithms were facilitated using a fast prototyping system, dSPACE1202, operating at a sampling rate of $T_s =$ 100 microseconds. The RL Agent block in MATLAB does not support Code Generation. However, enhancements have been made to the MATLAB Function Block to model SAC-DRL within Simulink. This modification permits the use of pre-trained networks, including reinforcement learning policies, for inference within Simulink. Consequently, this advancement enables the implementation of SAC-DRL in dSPACE1202 through code generation. For the initial synchronization of the inverter with an established grid voltage, a PLL is required, and then, after synchronization, a transition into GFM control is executed. It should be noted that the transition process is not mandatory because the synchronous power controller embedded in the active power loop naturally possesses the ability to synchronize. In this study, the transition approach is employed as a procedural measure in experimental tests to facilitate a soft start.

Fig. 3(a)–(c) shows the experimental comparisons (P, Q, i_{oa}) when P_r steps from 600 W to 1000 W at $t = 2s$ and Q_r steps from 100 to 300 VAr at $t = 7s$ in a stiff-grid connection (SCR = 8.66, estimated by grid inductance L_g). The proposed SAC-DRL-based grid impedance shaping method enhances

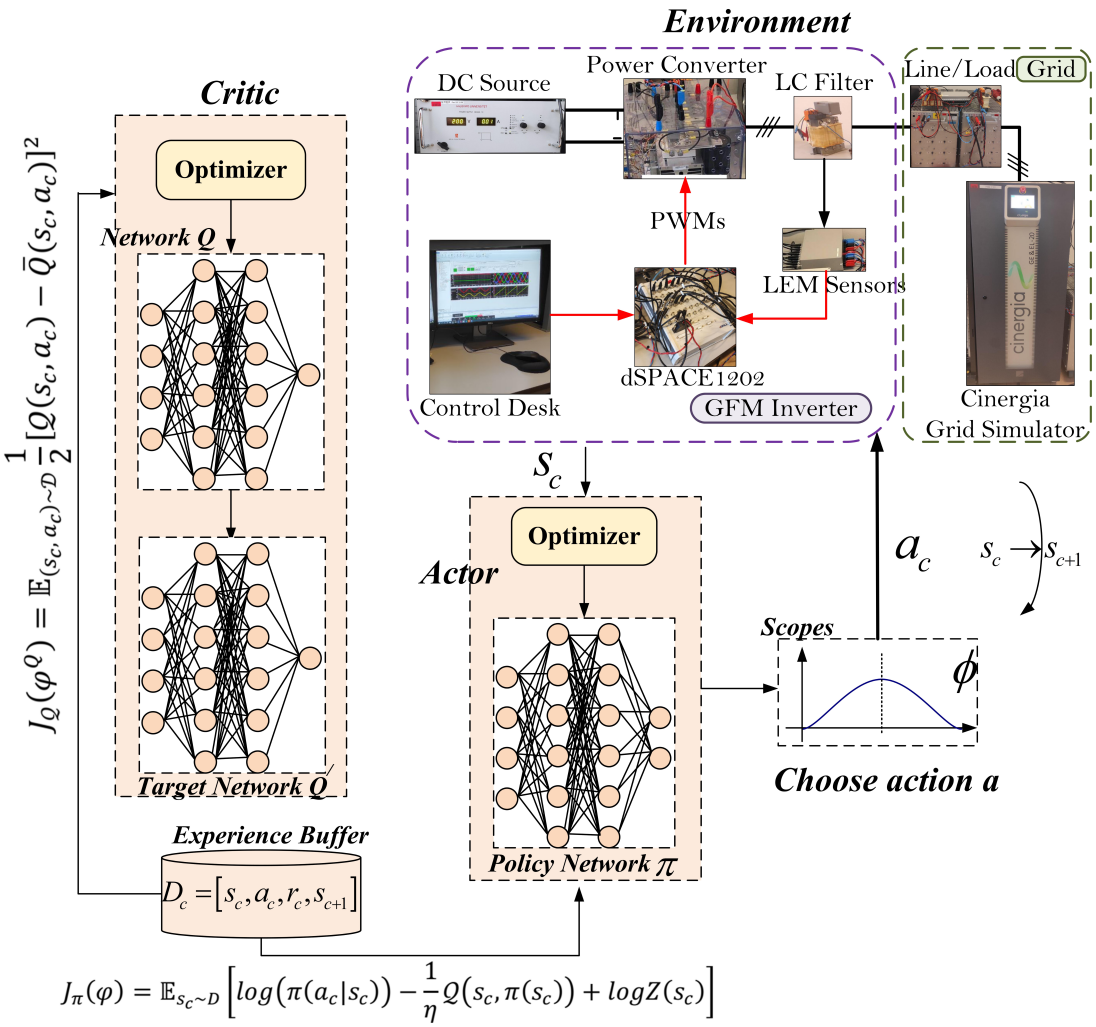

Fig. 2. Schematic of SCA-DRLA applied to GFM inverter.

TABLE I
MAIN PARAMETERS OF GFM INVERTER SETUP

l_g, r_g	L_f, C_f	S_r	V_{dc}	f_{SW}	v_g	ω_o
5.4 mH and 0.2 Ω	2.4 mH and 15 μF	1 kW	200 V	20 kHz	70 RMS	$100\pi rad/s$

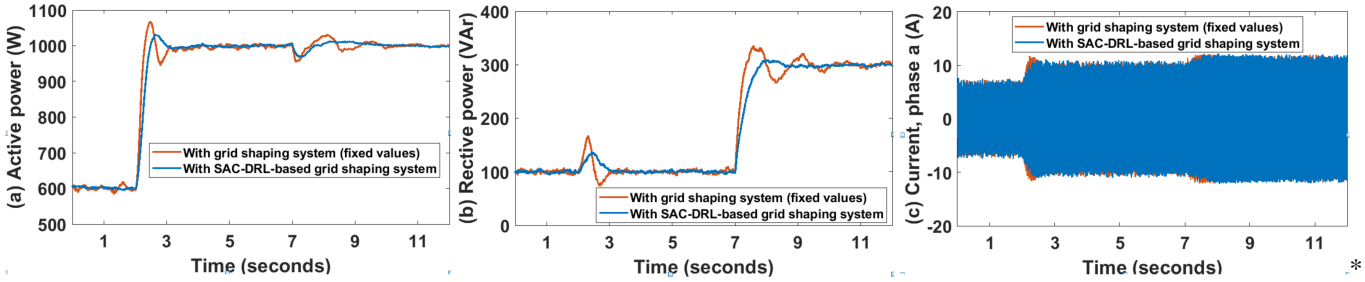

Fig. 3. Step responses with/without the proposed grid shaping system when SCR=8.6, P_r: 600 W to 1000 W, and Q_r steps from 100 VAr to 300 VAr: (a) active power; (b) active power; and (c) current.

oscillation damping and delivers faster and smoother dynamics, while also effectively reducing overshoot instances caused by power step insertions, compared to the virtual impedance implementation with fixed values ($r_{vi} = 0.38$, $x_{vi} = 1.4$). Fig. 4(a)–(c) compares the system's performance with SCR = 2.88 and an step change of 400 W in P_r at $t = 5s$. The

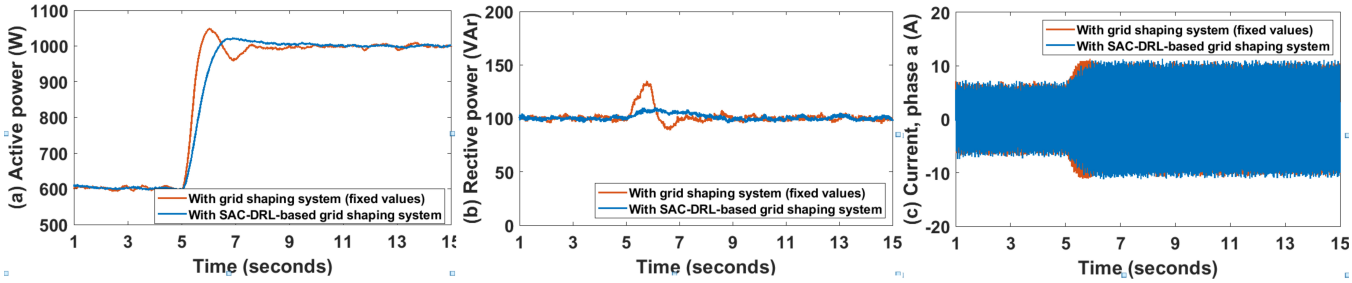

Fig. 4. Step responses with/without the proposed grid shaping system when SCR=2.88 and P_r: 600 W to 1000 W: (a) active power; (b) active power; and (c) current.

findings also indicate that the power coupling is substantially lower with the proposed strategy compared to stronger grids such as Fig. 3(a)–(b).

IV. Conclusion

This paper proposed an intelligent method for adjusting grid impedance in GFM inverters through the SAC-DRLA. This advanced approach combines dynamic virtual impedance control with an equivalent grid impedance estimator. It enables precise and adaptive adjustments to virtual impedance based on the grid's X/R ratio and the converter's power capacity, ensuring optimal power flow and maintaining grid stability, even amid impedance fluctuations. The introduced SAC-DRL-based strategy significantly improves oscillation damping and ensures more rapid and fluid dynamic responses. Furthermore, it adeptly minimizes the occurrence of overshoots resulting from sudden power changes, highlighting its efficacy in enhancing grid operation and stability.

V. Acknowledgment

This work was supported by the Reliable Power Electronic-Based Power Systems (REPEPS) project and the "SMART BATTERY" project (project number 222860), both hosted at the AAU Energy Department, Aalborg University, and part of the Villum Investigator Program funded by the Villum Foundation.

References

[1] R. L. d. A. Ribeiro, A. Oshnoei, A. Anvari-Moghaddam and F. Blaabjerg, "Adaptive Grid Impedance Shaping Approach Applied for Grid-Forming Power Converters," in IEEE Access, vol. 10, pp. 83096–83110, 2022.

[2] A. Oshnoei, S. Peyghami, H. Mokhtari, and F. Blaabjerg, "Grid synchronization for distributed generations," *Encyclopedia of Sustainable Technologies*. Elsevier, pp. 1–21, 2023.

[3] Y. Han, H. Li, P. Shen, E. A. A. Coelho and J. M. Guerrero, "Review of active and reactive power sharing strategies in hierarchical controlled microgrids," *IEEE Trans. Power Electron.*, vol. 32, no. 3, pp. 2427–2451, Mar. 2017.

[4] L. Ding, Q.-L. Han and X.-M. Zhang, "Distributed secondary control for active power sharing and frequency regulation in islanded microgrids using an event-triggered communication mechanism," *IEEE Trans. Ind. Informat.*, vol. 15, no. 7, pp. 3910–3922, Jul. 2019.

[5] J. M. Guerrero, J. C. Vasquez, J. Matas, L. G. de Vicuna and M. Castilla, "Hierarchical control of droop-controlled AC and DC microgrids—A general approach toward standardization," *IEEE Trans. Ind. Electron.*, vol. 58, no. 1, pp. 158–172, Jan. 2011.

[6] J. He, Y. W. Li and F. Blaabjerg, "An enhanced islanding microgrid reactive power, imbalance power, and harmonic power sharing scheme," *IEEE Trans. Power Electron.*, vol. 30, no. 6, pp. 3389–3401, Jun. 2015.

[7] C. Dou, Z. Zhang, D. Yue and M. Song, "Improved droop control based on virtual impedance and virtual power source in low-voltage microgrid," *IET Gener. Transmiss. Distrib.*, vol. 11, no. 4, pp. 1046–1054, Mar. 2017.

[8] H. Han, X. Hou, J. Yang, J. Wu, M. Su and J. M. Guerrero, "Review of power sharing control strategies for islanding operation of AC microgrids," *IEEE Trans. Smart Grid*, vol. 7, no. 1, pp. 200–215, Jan. 2016.

[9] B. Liu, Z. Liu, J. Liu, R. An, H. Zheng and Y. Shi, "An adaptive virtual impedance control scheme based on small-AC-signal injection for unbalanced and harmonic power sharing in islanded microgrids," *IEEE Trans. Power Electron.*, vol. 34, no. 12, pp. 12333–12355, Dec. 2019.

[10] D. K. Alves, R. L. d. A. Ribeiro, F. B. Costa, T. d. O. A. Rocha and J. M. Guerrero, "Wavelet-based monitor for grid impedance estimation of three-phase networks," *IEEE Trans. Ind. Electron.*, vol. 68, no. 3, pp. 2564–2574, Mar. 2021.

[11] F. Zhao, X. Wang and T. Zhu, "Power Dynamic Decoupling Control of Grid-Forming Converter in Stiff Grid," *IEEE Transactions on Power Electronics*, vol. 37, no. 8, pp. 9073–9088, Aug. 2022, doi: 10.1109/TPEL.2022.3156991.

[12] A. Oshnoei, H. Sorouri, R. Teodorescu and F. Blaabjerg, "An Intelligent Synchronous Power Control for Grid-Forming Inverters Based on Brain Emotional Learning," *IEEE Transactions on Power Electronics*, vol. 38, no. 10, pp. 12401–12405, Oct. 2023.

[13] A. Oshnoei, S. Peyghami and F. Blaabjerg, "Intelligent Control Approach Applied for Grid-Forming Power Converters," *2023 IEEE Applied Power Electronics Conference and Exposition (APEC)*, Orlando, FL, USA, 2023, pp. 3013–3019, doi: 10.1109/APEC43580.2023.10131254.

[14] A. Oshnoei, R. L. A. Ribeiro, A. Anvari-Moghaddam and F. Blaabjerg, "Learning-based Grid Impedance Shaping Method Applied for High-Accuracy Power Hardware-in-the-Loop," *2023 11th International Conference on Power Electronics and ECCE Asia (ICPE 2023 - ECCE Asia)*, Jeju Island, Korea, Republic of, 2023, pp. 2543–2548, doi: 10.23919/ICPE2023-ECCEAsia54778.2023.10213962.

[15] A. Fathollahi et al., "Robust Artificial Intelligence Controller for Stabilization of Full-Bridge Converters Feeding Constant Power Loads," *IEEE Transactions on Circuits and Systems II: Express Briefs*, vol. 70, no. 9, pp. 3504–3508, Sept. 2023, doi: 10.1109/TCSII.2023.3270751.

[16] Y. Zheng et al., "Load frequency active disturbance rejection control for multi-source power system based on soft actor-critic," " *Energies*, vol. 14, no. 16, p. 4804, 2021.